NEW SECTOR 37 CHAMBER DESIGN AND INSTALLATION FOR HIGH-CURRENT OPERATION OF THE APS STORAGE RING*

Y.-C. Chae, L. Morrison, J. Hoyt, W. Berg, R. Bechtold, L. Erwin, M. Givens,
K. Schroeder, R. Soliday, J. Stevens, G. Waldschmidt
Argonne National Laboratory, Argonne, IL 60439, USA

Abstract

The Advanced Photon Source (APS) is a 7-GeV hard x-ray synchrotron light source consisting of 40 sectors. Sector 37 accommodates four radio-frequency cavities followed by a short straight section, which is set aside for the future installation of a diagnostic device. The 77.2-cm-long section of spool pieces can be isolated by two gate valves and have an independent vacuum pump. The spool pieces are normally under high vacuum condition when the total current is below 100 mA. However, at the higher current required for the APS Upgrade, rf heating causes an unacceptable rise in temperature. We analyzed this situation by wakefield simulation, which led to a new chamber design. Proper fabrication and careful installation with twelve thermocouples ensured a temperature rise under 40-50°C at 100 mA. A brief thermal analysis showed that the present observed temperature rise in the new chamber is mainly due to the resistive wall.

INTRODUCTION

During APS Run 2011-1 we discovered the horizontal scraper at sector 37 was damaged. We also found that the slotted screen in the vertical vacuum tee was mechanically distorted. As a result, we pulled out the scraper and replaced it with a bellow. The layout of sector 37 (S37SS) during Run 2011-2 is shown in Figure 1; the space can be isolated by two gate valves.

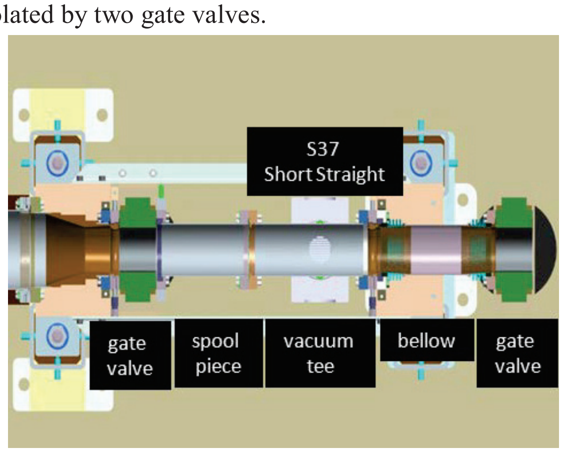

Figure 1: The old layout of sector 37 short straight used during Run 2011-2.

During Run 2011-2 we still experienced a temperature rise to 100°C and above with the stored current at 100 mA in 24-singlet mode of operation (24S). The location of the highest temperature was near the pumping port of the vertical tee. This limited the total current below 100 mA even though we sometimes needed to operate the ring above 100 mA. We were thus motivated to perform a thermal analysis of S37SS.

Since the temperature rise was caused by rf heating, we performed the impedance analysis of S37SS and identified two problem areas that needed improvement. The mitigation to the problem was found and, subsequently, a new design was proposed. The new S37SS was installed for Run 2011-3. After a brief commissioning, we readily determined that S37SS was cool enough to lift the ban on the 100-mA beam current limit in 24S.

In this paper we report the impedance analysis of S37SS chambers and its performance at the storage ring.

S37SS DURING RUN 2011-2

The APS storage ring provides users with three different fill patterns; among them is 24S and 324S, which consist of 24 and 324 bunches, respectively, equally spaced around the ring. We keep the current constant in 24S via top-up injection every two minutes; whereas the ring is on fill-on-fill mode for 324S to compensate for the particles lost due to finite lifetime. The difference in fill pattern has a significant effect on the chamber temperature: for the same total current in the ring, the amount of energy lost by the beam due to wakefield interaction is inversely proportional to the number of bunches in the ring.

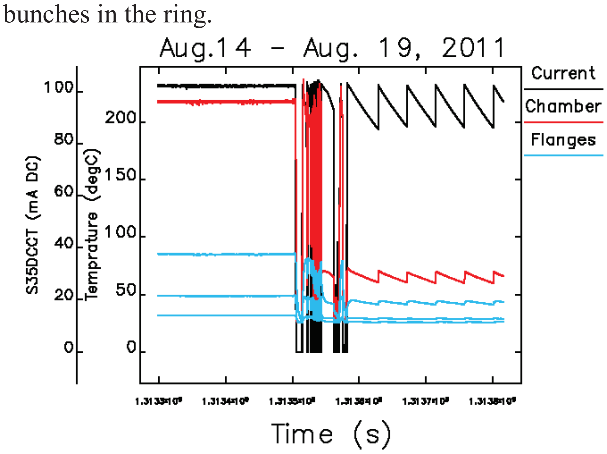

Figure 2: Chamber temperature measured during Run 2011-2. The constant current was maintained by top-up injections in 24S and the saw-tooth-like current decay is in 324S.

In order to understand the high temperature in Figure 2, we modeled S37SS with GdfidL [1], as depicted in Figure 3. The spool piece and vacuum tee along the beam

*Work supported by U.S. Department of Energy, Office of Science, under Contract No. DE-AC02-06CH11357.

ISBN 978-3-95450-115-1

direction from left to right is a circular chamber; together with the end wall, it forms a pill-box cavity connected to the elliptical pipe with aperture in (a,b) = (4.2 cm, 2.1 cm). The vertical tee is attached to a 5-cm-diameter pumping port.

Figure 3: The model used in GdfidL.

The longitudinal wake potentials were computed with and without vertical tee as shown in Figure 4. Without tee the wake does not decay even after the beam passed the structure by 100 m. This long-range wake causes the coupled-bunch instability as well as the resonance heating. With a tee we see an interesting phenomenon that shows the damping over the distance; a similar mechanism was used for the high-order mode (HOM) damping in the APS 352-MHz cavity. As is well known, the temperature rise in a HOM damper often limits cavity operation. Hence, this explains the high temperature around the pumping port.

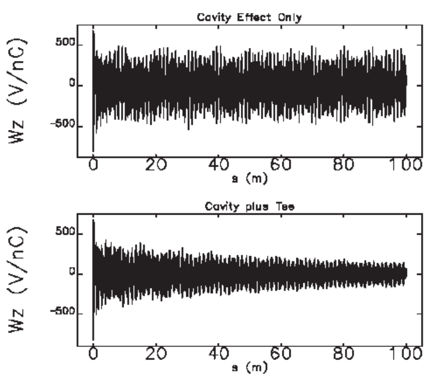

Figure 4: The longitudinal wake potentials of the old S37SS without (top) and with (bottom) the vertical tee.

The energy change of a bunch of charge q is

$$\Delta E = k_z q^2, \tag{1}$$

where k_z is the loss factor that GdfidL computes for the chamber. Then, the power lost by the beam in the ring is

$$P[Watt] = \frac{I[A]^2}{N_b \times f[Hz]} k_z[V/C], \tag{2}$$

where I is total current, N_b is the number of bunches, and f is the revolution frequency. This is a parasitic beam loss that causes rf heating. We found that the loss is 768 W and 734 W with and without the tee, respectively, if the 100-mA beam is stored in 24S. This implies that most of the parasitic loss is caused by the cavity-like chamber; the tee does not add much of its own wake to the total loss.

NEW S37SS CHAMBER DESIGN

The obvious design choice is the removal of the cavity effect by matching the spool-piece aperture to the elliptical pipe. This alone reduced the loss from 768 W to 160 W. The configuration is shown in Figure 5(a). Since the aperture is matched, the only source of impedance is the vertical tee. It only contributed a modest amount of beam loss when it was part of the old S37SS in Figure 3, but it now acts as a large impedance source in the Figure 5(a) configuration even though the vertical tee is unchanged.

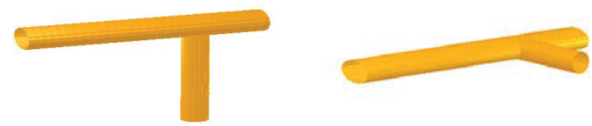

(a) (b)

Figure 5: The chamber for the spool-piece and vacuum tee is matched to the regular APS chamber in (a,b)=(4.2 cm, 2.1 cm). The orientation of the tee can be either vertical in 5(a) or horizontal in 5(b).

For the loss factor analysis we use the formula developed for the broadband resonator impedance as [2]

$$k_z = \frac{R_s}{4\sqrt{\pi} Q^2 \omega_r^2 \sigma_z^3}. \tag{3}$$

The resonator parameter that appeared in Eq. (3) was found in [3]; that is, for a hole of radius d, Q=1.8, ω_r=1.35(c/d), and R_s=0.216Z_0(d/b)^2, where b is the distance between the beam and the hole. Then, the loss factor in Eq. (3) scales as

$$k_z \propto d^4 / b^2. \tag{4}$$

Guided by Eq. (4), we turn the tee from vertical to horizontal as shown in Figure 5(b). By doing this, we naturally reduced the aperture of the pumping port from 5 cm to 4.2 cm, which is equal to the vertical height of the elliptical pipe. The combined effect is a reduction of the loss factor by a factor of 10 according to Eq. (4). The actual computation by GdfidL for the bunch length σ_z = 1 cm showed the loss factor improved by a factor of 40. That, in turn, reduced the loss from 160 W down to 4 W for the 100-mA beam in 24S. The significant reduction in the wake potential that resulted from rotating the tee by 90 degrees is shown in Figure 6.

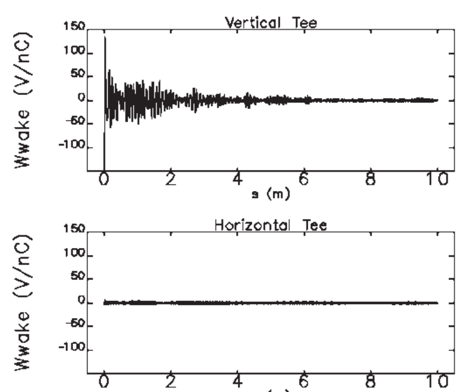

Figure 6: The wake potential of the vertical (top) and horizontal (bottom) tee, respectively, showing that the horizontal tee can reduce the rf heating significantly. Note that the vertical scales are the same.

S37SS DURING RUN 2011-3

Guided by the above analysis, we designed and fabricated the chamber and pump-out tee during the shutdown period. The newly installed chambers are shown in Figure 7. The thirteen thermocouples are installed for the thermal analysis whose layout is shown in Figure 8. The temperature was monitored during Run 2011-3. As the current increased to 100 mA the thermocouples recorded the temperature along the S37SS chambers; the result is shown in Figure 9. Depending on the location of the thermocouple, the temperature ranges from 40°C to 50°C at 100 mA. This temperature was a result of equilibrium between the cooling and heating rates.

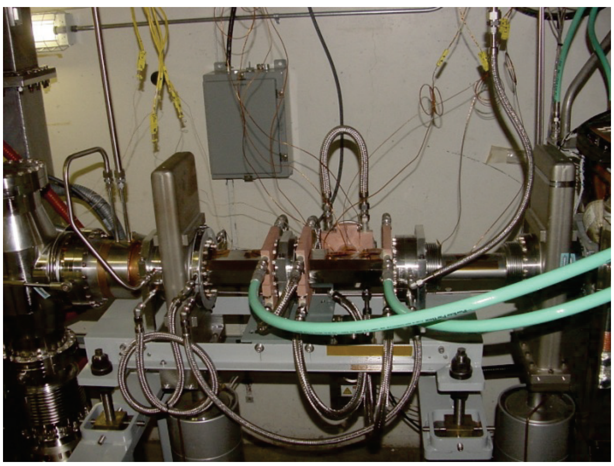

Figure 7: The new S37SS chamber is installed in August of 2011 between two gate valves. The clamps around the chamber were connected to the cooling system, but, that was not used and later removed off the S37SS. The Kapton tape on the surface shows location of the thermocouples.

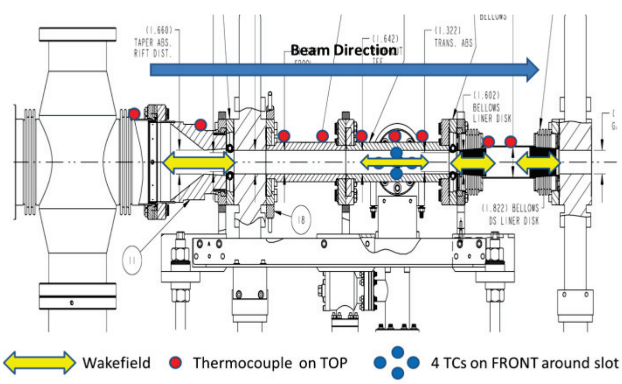

Figure 8: The layout of the thermocouples.

The cooling is estimated by using the Newton's cooling law:

$$q = hA\left(T_w - T_\infty\right), \tag{5}$$

where q is a cooling rate, h is a convection heat transfer coefficient, T_w is the surface temperature, and T_∞ is the ambient temperature. If we assume a natural convection by buoyancy, the heat transfer coefficient h is a function of the Prandtl number Pr and Grashof number Gr. That is [4],

$$h = 0.53\left(Gr\,\mathrm{Pr}\right)^{1/4}\frac{k}{d}, \tag{6}$$

where k is the thermal conductivity of material, and d is the diameter. When we used T_w = 40°C, T_∞ = 26°C, and d = 6 cm, the computed value of h becomes 5.327 W/m^2/°C that resulted in the cooling rate q = 14 W/m. In this estimation we assume a 1-m-long circular tube with the temperature at T_w.

The heating by the beam has two sources: one by the geometric impedance and the other by resistive wall impedance. For a cylindrical resistive wall with conductivity σ_c and pipe radius b, the loss factor per unit length for a Gaussian bunch is [2]

$$\frac{k_z}{L} = \frac{1.225c}{4\pi^2 b\sigma_z^{3/2}}\left(\frac{Z_0}{2\sigma_c}\right)^{1/2}. \tag{7}$$

Together with Eq. (2) we estimated that the resistive wall contributes 10 W/m. Since we know that the parasitic loss by the beam due to geometric impedance is less than 4 W/m, the total heating by a 100-mA beam in 24S then will be less than 14 W/m. From this we conclude that the moderate temperature rise is mainly caused by the resistivity of 316L stainless steel.

The thermal analysis based on free convection cooling explains a moderate temperature rise to about 40°C observed during Run 2011-3.

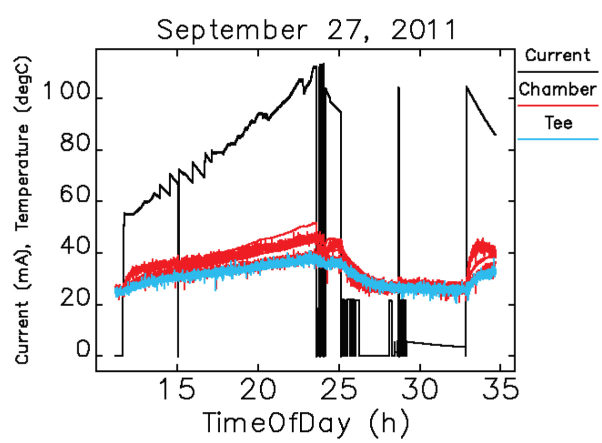

Figure 9: Temperature measurement during 2011 Run-3 with the new S37SS chambers installed. This must be compared with the temperature in Figure 2.

REFERENCES

[1] W. Bruns, Proc. LINAC2002, p. 418 (2007); http://www.JACoW.org
[2] A. Chao, M. Tigner, *Handbook of Accelerator Physics and Engineering*, 2nd Printing, (World Scientific Publishing, 2002), p. 212.
[3] Y.-C. Chae, Proc. PAC1995, p. 2995 (1995); http://www.JACoW.org
[4] J.P. Holman, *Heat Transfer*, 10th Edition (McGraw Hill), p. 327.